Geophysical Research Letters

RESEARCH LETTER
10.1029/2018GL079802

Key Points:
- Outstanding stratospheric and tropospheric conditions occurred in late winter 2018, with a persistent SSW and extreme Iberian precipitation
- The rainy conditions were associated with an extremely persistent negative NAO pattern
- The 2018 SSW played a relevant role in the shift to and maintenance of the negative NAO event that ended the severe Iberian drought

Supporting Information:
- Supporting Information S1

Correspondence to:
B. Ayarzagüena,
bayarzag@ucm.es

Citation:
Ayarzagüena, B., Barriopedro, D., Garrido-Perez, J. M., Abalos, M., de la Cámara, A., García-Herrera, R., et al. (2018). Stratospheric connection to the abrupt end of the 2016/2017 Iberian drought. *Geophysical Research Letters*, *45*, 12,639–12,646. https://doi.org/10.1029/2018GL079802

Received 27 JUL 2018
Accepted 12 NOV 2018
Accepted article online 16 NOV 2018
Published online 29 NOV 2018

Stratospheric Connection to the Abrupt End of the 2016/2017 Iberian Drought

B. Ayarzagüena[1,2], D. Barriopedro[2], J. M. Garrido-Perez[1,2], M. Abalos[1], A. de la Cámara[1,2], R. García-Herrera[1,2], N. Calvo[1], and C. Ordóñez[1]

[1]Departamento de Física de la Tierra y Astrofísica, Universidad Complutense de Madrid, Madrid, Spain, [2]Instituto Geociencias, CSIC-UCM, Madrid, Spain

Abstract Southwestern Europe experienced extraordinary rainy and windy conditions in March 2018, leading to the end of the most severe drought since 1970 at continental scale. This anomalous weather was linked to a persistent negative North Atlantic Oscillation pattern. Two weeks earlier a sudden stratospheric warming (SSW) took place, preceded by the strongest planetary wave activity on record. In this study, we explore the connection between the SSW and the weather shift by employing a weather regime approach and flow analogues. The timing of the downward propagation of the stratospheric anomalies, the transition to and persistence of the negative North Atlantic Oscillation weather regime, and the sudden precipitation increase are all consistent with the typical tropospheric state after SSWs. Our results evidence a significant role of the 2018 SSW in the record-breaking precipitation event.

Plain Language Summary March 2018 was characterized by extraordinary heavy rain and strong winds over the Iberian Peninsula that ended the most severe drought since 1970 at continental scale. Two weeks earlier the polar stratosphere experienced anomalous conditions with a sudden rise in temperature, so-called sudden stratospheric warming (SSW). Although SSWs are not rare events, the 2018 case was remarkable in terms of its intensity and persistence. The coincidence in time of both extreme events and the known link between SSWs and anomalous weather in the North Atlantic led the media to claim that the SSW was the main culprit of the anomalous weather of March 2018. However, this assumption is not straightforward because of the large variability in the magnitude of tropospheric responses to SSWs. Here we explore the role of the SSW in the abrupt weather shift by analyzing the downward propagation of the SSW signal and its link to the tropospheric synoptic conditions. Our results indicate an actual connection between the 2018 SSW and the record-breaking precipitation event.

1. Introduction

In 2016/2017 western Europe suffered a prolonged drought with acute impacts on agriculture and energy production and devastating wild fires. This was the most severe drought at continental scale since at least 1970 (Garcia-Herrera et al., 2018). In southwestern Europe, the dry conditions lasted until the end of February 2018, when they were replaced by rainy weather that unusually persisted for almost a month. Precipitation anomalies were so extraordinary that hydroelectric water reservoirs and many river basins of the Iberian Peninsula recovered from a 20-year minimum in November–December 2017 to above normal values by the end of March 2018 (data from www.ree.es; Ministerio de Agricultura y Pesca, Alimentación y Medio Ambiente, 2018). The National Oceanic and Atmospheric Administration (NOAA) identified the anomalous precipitation of March 2018 over Spain as a significant climate event at global scale (National Oceanic and Atmospheric Administration, 2018). Wet conditions were also accompanied by strong winds. In Portugal, renewable energies, mainly hydroelectric energy and wind power, were able to cover the entire electric production for the first time in March 2018 (Associaçao Portuguesa de Energias Renováveis, 2018). Simultaneously, they also represented the largest contribution to the total electric power in Spain (52%; data from www.ree.es). Other European areas also experienced extreme weather. Snow hit Rome by the end of February (The Washington Post, 2018), and the United Kingdom suffered two episodes of very low temperatures and unusual snowfall in what the media called the *Beast from the East* (Met Office, 2018).

The shift to these weather conditions was timely with the occurrence of a sudden stratospheric warming (SSW) on 12 February 2018. SSWs are abrupt disruptions of the wintertime polar stratosphere whereby typical westerly winds are replaced by easterly winds. They occur twice every three boreal winters on average (Butler et al., 2015, Palmeiro et al., 2015) and are primarily driven by enhanced upward propagation of planetary wave activity (Matsuno, 1971). It is well known that after these events, stratospheric circulation anomalies can propagate downward into the troposphere, inducing a negative phase of the Northern Annular Mode (NAM)/North Atlantic Oscillation (NAO). During this phase, the NAO is associated with cooling in Eurasia and brings above-average precipitation to southwestern Europe (e.g., Kidston et al., 2015, and references therein). In this context, the 2018 SSW was claimed by the media (e.g., The Guardian, 2018) as the main culprit of the anomalous weather of March 2018 over Europe. However, there is still much uncertainty about the magnitude of the tropospheric response to SSWs since tropospheric conditions sometimes prevail over the stratospheric signal (Gerber et al., 2009). Thus, the connection between the weather shift over southwestern Europe and the 2018 SSW is far from being firmly established.

Here we use the record of SSWs in the satellite period and multiple approaches to investigate the role of the 2018 SSW in the abrupt end of the southwestern European drought in March 2018. To do so, after describing both tropospheric and stratospheric conditions, we address the following questions: Was there a traceable downward signal of the SSW to the troposphere, and was it timely with the weather shift? If so, to what extent did the SSW raise the probability of such weather conditions to occur?

2. Data and Methodology

We use daily mean data from the National Centers for Environmental Prediction/National Center for Atmospheric Research reanalysis at 2.5° × 2.5° horizontal resolution (Kalnay et al., 1996) and daily precipitation totals from the Climate Prediction Center Global Unified Precipitation dataset at 0.5° × 0.5° resolution (Xie et al., 2010). The analysis covers the period 1979–2018. The climatological daily mean is computed for the 1981–2010 period using a 31-day centered running mean. Anomalies are defined as departures of the daily fields from the filtered daily climatology.

The NAM is computed to identify the downward propagation of the SSW signal. It is defined as the first empirical orthogonal function (EOF) of the daily mean geopotential height anomalies poleward of 20°N. The EOF analysis is applied to each pressure level separately from 1,000 to 10 hPa and for the extended winters (1 December to 15 April) of the period 1979–2018 (Baldwin & Dunkerton, 2001). To characterize the tropospheric circulation over the Euro-Atlantic sector, we define four weather regimes (WRs) based on daily anomalies of geopotential height at 500 hPa (Z500). Following previous studies (Charlton-Pérez et al., 2018; Corti et al., 1999; Michelangeli et al., 1995), in order to smooth the data, we retain the 20 leading principal components of the extended winter daily Z500 anomalies over the Euro-Atlantic area (80°W to 50°E, 25–85°N). The 20 leading variability modes of Z500 account for more than 90% of the total variance in Z500. Then, a k-means clustering of four nodes is applied to the Z500 field reconstructed from these principal components, so that each day is assigned to one of these four clusters (Aurenhammer, 1991). The WRs correspond to the average of the anomalous Z500 fields for all days of each group (shown in supporting information Figure S1) and are labeled as Positive NAO (NAO+), Negative NAO (NAO−), Scandinavian blocking (SCAN Block), and Atlantic Ridge (ATL Ridge) regimes.

SSWs are identified using Charlton and Polvani (2007) criterion based on the reversal of zonal mean zonal wind at 60°N and 10 hPa. The onset date of each event corresponds to the first day that this condition is met. SSWs occurring from 15 December until the end of February are considered to ensure that only midwinter events are included in our computations. This way, stratospheric final warmings and very early SSWs are discarded.

Two-sample Kolmogorov-Smirnov (two-sample K-S) and Student's *t* tests are applied to assess the significance of results under the null hypothesis of equal distributions and equal means, respectively (Wilks, 2011). When required, confidence intervals are computed for SSW-related estimates by using a bootstrap of 1,000 trials, each containing a random selection (with replacement) of the same number of events among those of the 1979–2017 period. In addition, the study uses fitted probability distributions to simplify the representation of the duration of NAO− events and the wintertime precipitation over Iberia. For that purpose, we adopt the nonparametric technique of Gaussian kernel density estimation (Pedregosa et al., 2011; Rosenblatt, 1956) with a Scott's bandwidth method.

3. Results

First, we examine the monthly tropospheric conditions over the Euro-Atlantic area in March 2018 (Figures 1a and 1b). Iberia was the most affected region, with anomalies larger than 1.5 standard deviations of the monthly climatology. Strong westerly winds exceeded the average value by 4 m/s, and mean precipitation anomalies were larger than 6 mm/day in many areas, with accumulated totals for March hitting record values. The extraordinary windy conditions were consistent with the largest contribution of wind power to the energy production of that month since data are available in Spain (1990; data from www.ree.es). Cold temperature anomalies over Iberia, although not as large as wind and precipitation anomalies, exceeded 2 °C and occurred simultaneously with abundant precipitation. This resulted in an anomalous amount of snow, even in areas of Iberia where it is unusual (not shown).

These anomalies are consistent with a large-scale sea level pressure pattern (contours in Figure 1a) which resembles the negative phase of the NAO. The link between the anomalous conditions of March 2018 in Iberia and the atmospheric circulation can be analyzed in more detail by using the WRs (see details in section 2). The daily sequence of WRs over the Euro-Atlantic area from 1 January to 31 March 2018 is shown in Figure 1c in colors. During the first two months of 2018, different WRs followed one another with prevalence of SCAN Block. All WRs are typically associated with near- or below-normal precipitation in Iberia (Figure S1), except for NAO−, which was not very frequent during these two months. Consequently, the accumulated precipitation since 1 October 2017 (the beginning of the hydrological year in Iberia) remained well below the climatological mean. As a result, the previous drought conditions went on until the late winter. In contrast, at the end of February a NAO− pattern settled in and persisted throughout most of March. This WR is associated with negative anomalies of geopotential height over the eastern Atlantic and enhanced precipitation in southern Europe, particularly in Iberia (Figure S1c). Consistently, the shift to NAO− coincided with a rapid rise of the accumulated precipitation (blue line in Figure 1c). The NAO− WR was extremely persistent (21 days, Figure 1c), lying beyond the 98th percentile of the climatological distribution of winter NAO− events. Accumulated precipitation rose up to near-normal values by the middle of March 2018 (solid black line in Figure 1c) and beyond the 75th percentile at the end of that month (upper gray dashed line in Figure 1c).

As stated in section 1, NAO− events are a common fingerprint of SSWs, but was the 2018 SSW also exceptional? Figure 2a presents the evolution of the zonal mean zonal wind at 10 hPa and 60°N during the entire winter. The polar night jet decelerated abruptly at the beginning of February, and the mean flow became easterly on 12 February. In the following days, these easterly winds reached the highest values ever measured at that time of the year. They were also very persistent (16 days) in comparison with the average duration of easterly winds during SSWs (7.6 ± 1.9 days). The total eddy heat flux at 100 hPa in early February was also the strongest ever recorded in the extended winter season (Figure 2b). In terms of anomalous eddy heat flux before the SSW, the 10-day average value in 2018 reached 30.9 K m/s, considerably larger than for any other SSW of the 1979–2017 period (average value and its standard error: 11.9 ± 1.3 K m/s) (Figure 2c). This was mainly due to the wave number 2 (WN2) component, which exceeded the maximum values prior to any other SSW (Figure 2d). In contrast, the wave number 1 (WN1) component was close to the minimum values on record. This is consistent with the split of the polar vortex into two pieces around the onset date of the SSW (Figure S2).

To explore the links between the extraordinary Iberian precipitation event and the 2018 SSW, we first analyze the evolution of the NAM index during that winter (Figure 1d). In the middle stratosphere (10 hPa), the SSW is easily identified by negative NAM values starting in mid-February. The signal descended with time and reached the lower stratosphere by the end of the month, where it persisted over approximately 30 days (80th percentile of the distribution of NAM events at 200 hPa). The downward propagation of the SSW-related NAM signal was confirmed by using the tracking algorithm by Palmeiro et al. (2015) and the criterion to identify propagating SSWs by Karpechko et al. (2017). By the end of February, there are also strong and persistent negative values of the NAM index in the troposphere, especially near surface, in agreement with Figures 1a and 1c. The arrival of the negative NAM signal to the troposphere coincides in time with the WR shift to NAO−, pointing out a stratospheric influence. This result agrees well with Hitchcock and Simpson (2014), who showed that the NAM-like tropospheric response to SSWs occurs timely with the lower-stratospheric NAM anomalies and not with the onset date of the SSW. The strong persistence of

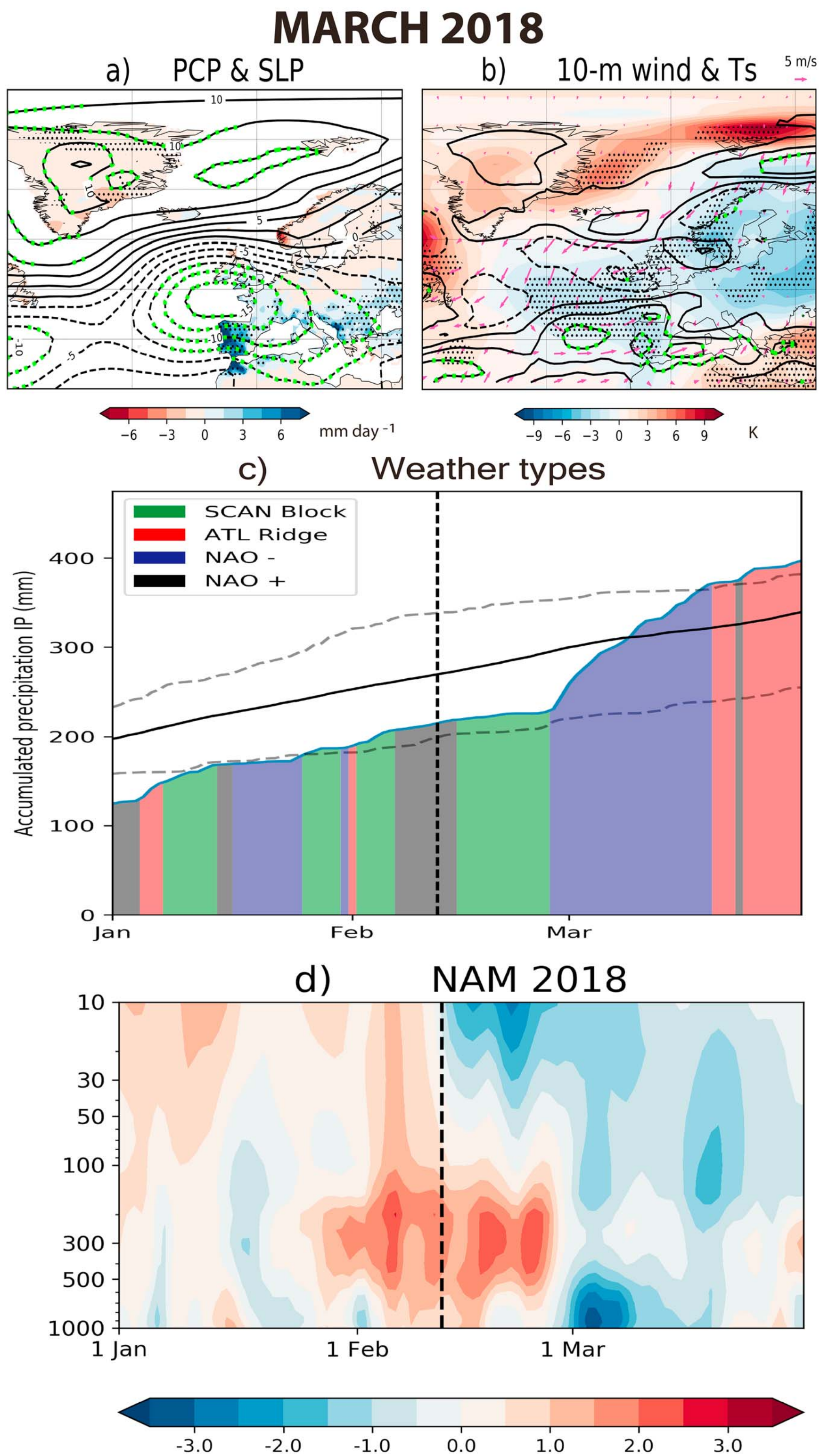

Figure 1. March 2018 anomalies of (a) SLP (hPa, contours) and precipitation (mm/day, shading), (b) 10-m wind (vector field in arrows, wind magnitude as 2-m/s contour intervals)) and 2-m temperature (K, shading). Green contours (hatching) in (a) and (b) denote anomalies larger than ±1.5 standard deviations for the variables displayed in contours (shading). (c) Daily evolution of weather regimes (color bars) and accumulated precipitation since 1 October 2017 over Iberia (blue line). Gray dashed lines indicate the 25th and 75th percentiles, and black line represents the climatological value. (d) Daily evolution of standardized NAM index for the 2018 winter at different pressure levels. The vertical dashed lines in (c) and (d) depict the onset of the 2018 SSW. SLP = sea level pressure; PCP = precipitation; ATL Ridge = Atlantic Ridge; NAO = North Atlantic Oscillation; NAM = Northern Annular Mode; SSW = sudden stratospheric warming.

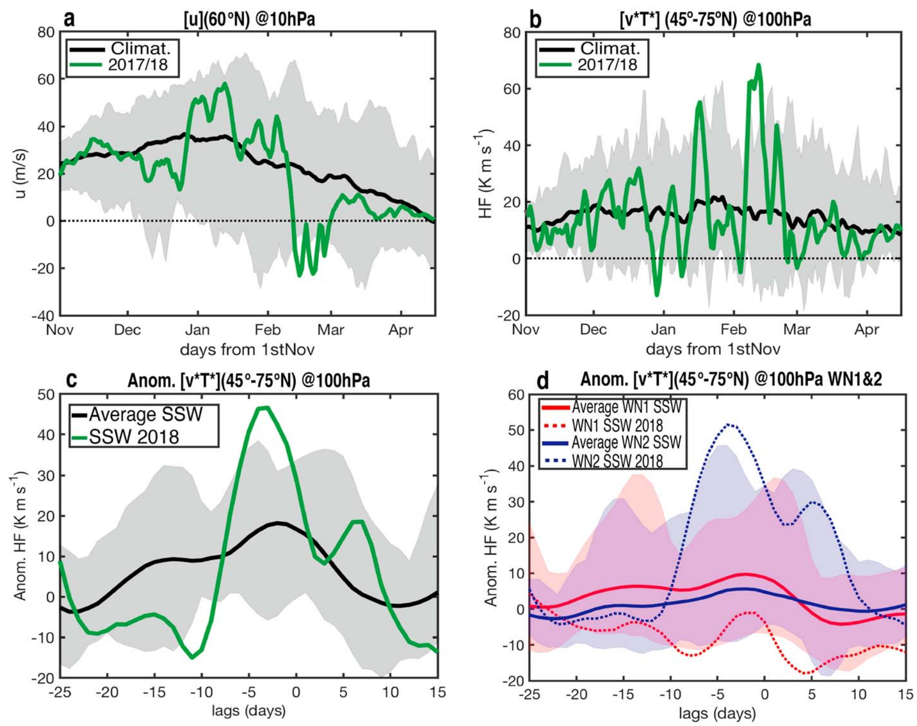

Figure 2. (a) Time series of zonal mean zonal wind at 10 hPa and 60°N from 1 November 2017 to 15 April 2018 (green line). Black solid line corresponds to the daily mean for the period 1981–2010. (b) Same as (a) but for the area-weighted meridional eddy heat flux at 100 hPa averaged over 45–75°N. (c) Time evolution of anomalous extratropical eddy heat flux at 100 hPa during the 2018 event (green line) and for all SSWs in 1979–2017 (black solid line), with the zero lag (*x* axis) indicating the onset of SSWs. (d) Same as (c) but for the WN1 (red) and the WN2 (blue) components of the extratropical eddy heat flux at 100 hPa. Shadings cover the interval between the daily maximum and minimum of each field for the period 1979–2017. Data in (c) and (d) were smoothed with a 5-day running mean. SSW = sudden stratospheric warming.

negative NAM values in the lower stratosphere is typical of SSWs (Gerber et al., 2009) and consistent with that of a negative NAO in the troposphere, supporting the role of the 2018 SSW in promoting the transition to and the persistence of the NAO− regime.

Next, we analyze whether the observed WRs during the 2018 SSW are typically found during the lifetime of SSWs. To do so, the most frequent WRs during the pre-SSW (−15/0 days) and post-SSW (+8/+40 days) periods of all SSWs from 1979 to 2017 are identified and compared to those of 2018 (Figure 3a). Note that these periods are not contiguous since we have allowed some time (8 days) for the stratospheric signal to descend to the troposphere, as in Karpechko et al. (2017). Nevertheless, the results are robust to changes in the definition of the post-SSW period (see Figure S3). The large spread in the distribution of WRs in both periods (pre-SSWs and post-SSWs) reflects the diversity of precursors of SSWs already reported in previous studies (e.g., Cohen & Jones, 2011; Garfinkel et al., 2010), as well as the uncertainty in the tropospheric response to SSWs (Gerber et al., 2009). Still, the most likely WR prior to SSWs is the SCAN Block, with higher frequencies than the other WRs. This result agrees well with the preferred location of blockings that enhance upward propagating wave activity (Barriopedro & Calvo, 2014; Nishii et al., 2011). More specifically, some studies have identified an increased frequency of SCAN Block prior to WN2 SSWs (Cohen & Jones, 2011; Nishii et al., 2011), as is the case of the 2018 SSW. During the post-SSW period, NAO− is the most frequent WR (Figure 3a), even when it only explains 18.7% of the Z500 variance in winter (compared to more than 23% for each of the other WRs, Figure S1). The predominance of NAO− after SSWs agrees with Charlton-Pérez et al. (2018) and provides additional evidence for a relevant stratospheric role in inducing the 2018 NAO− WR. Green stars in Figure 3a indicate that the predominant WRs before and after the 2018 SSW coincide with the preferred ones for other SSWs, supporting the stratospheric contribution to WRs in late winter 2018. The enhanced frequency of NAO− after the 2018 SSW is an outlier in the distribution of SSWs, consistent with the long-lasting signatures of the 2018 SSW in the stratosphere and with the long duration of the NAO− in March 2018.

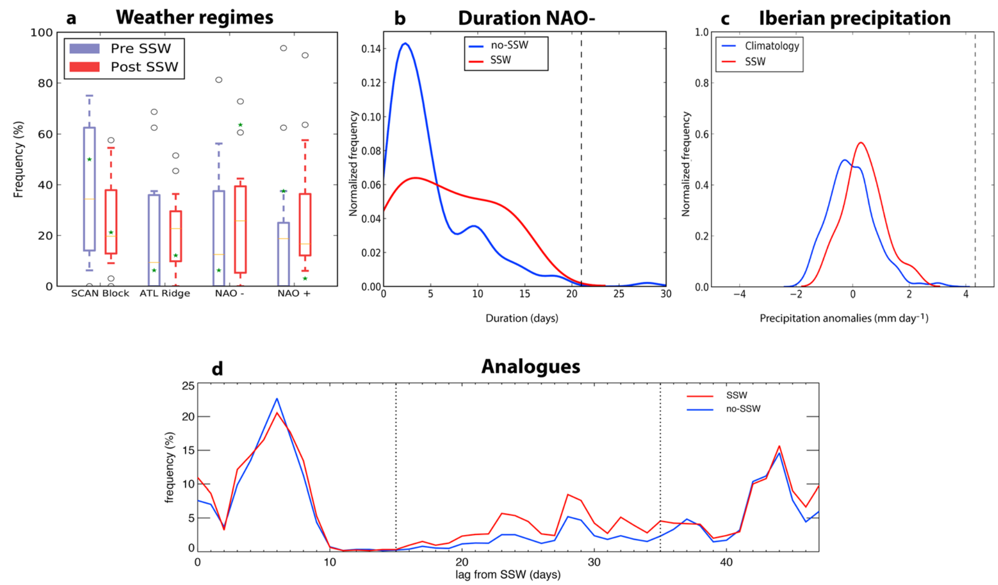

Figure 3. (a) Frequency (%) distribution of weather regime days for −15/0 days prior to SSWs (purple) and +8/+40 days after SSWs (red). Orange lines show the median, the whiskers extend from 10th to 90th percentiles, empty circles indicate values beyond the [10th, 90th] percentile range, and green stars correspond to the 2018 SSW. (b) Fitted probability distribution of NAO− duration (in days) for events that happen within +8/+40 days after SSWs (red line) and for the remaining ones (blue line). Vertical dashed line indicates the value for the 2018 SSW. (c) Same as (b) but for Iberian precipitation anomalies (mm/day) for the post-SSW period (red line) and a climatology built from a random selection of 33-day blocks from January–March of 1981–2010 similar to the procedure followed for SSWs (blue line). (d) Frequency of good flow analogues (in percent of winter days of 1979–2017) of the 2018 post-SSW period during days following a SSW (red) and the remaining winter days (blue). Vertical dashed lines delimit the 2018 NAO− event. See text for details. SSW = sudden stratospheric warming; NAO = North Atlantic Oscillation.

The mentioned long duration of the NAO− WR is then another characteristic of the March 2018 event that points to an influence of the SSW. Indeed, we have confirmed that the probability of a NAO− event persisting longer than 5 days rises from 40.0% in the climatology to 65.2% under the influence of a SSW, with the former being out of the 95% confidence interval of the later ([43.5%, 82.6%]) according to a 1,000-trial bootstrap. This is illustrated in Figure 3b. The distribution of the NAO− persistence following SSWs (red line) is flatter and shifted toward higher values as compared to the remaining NAO− events (blue line). Both distributions are significantly different at the 97.5% confidence level (two-sample K-S test). Figure 3b stresses again the exceptionality of the 2018 NAO− event (vertical dashed line), whose duration is at the very end of the upper tails of the distribution.

The unusual persistence of NAO− following the 2018 SSW contributes to explaining the record-breaking precipitation observed in Iberia. Figure 3c reveals that the climatological distribution of precipitation anomalies in winter (blue line) shifts toward positive values after SSWs (red line). This change is statistically significant at the 98% confidence level (two-sample K-S test). When a SSW happens, the probability of above-normal precipitation (76.5% with a 95% confidence interval of [52.9%, 94.1%]) is significantly higher than the climatology (44.8%). Therefore, although exceptional (see vertical dashed line in the figure), the precipitation anomalies registered in 2018 were qualitatively consistent with the occurrence of the SSW.

Finally, we use the analogue method to find synoptic conditions among the winters of 1979–2017 that were similar to those experienced during the 2018 event. For each day from the SSW onset until the end of March 2018 (+47 days after the 2018 SSW), we counted the number of good analogues found in the reanalysis period (excluding that winter). They are defined as those days with root-mean-square error of the anomalous Z500 field over (30°W to 15°E, 30–55°N), with respect to the same field during the mentioned 47 days, below their 5th percentile (Jézéquel et al., 2018). To identify a stratospheric influence, the search was separated into winter days after SSWs (with SSWs, from now on) and the remaining winter days of 1979–2017 (without SSWs, hereafter). The evolution of good analogues along the 2018 winter reveals that the NAO− event was bounded by two intervals with high frequency of good analogues, indicating relatively common synoptic conditions (Figure 3d). This frequency is similar for winter periods with and without SSWs. Thus, weather conditions observed before and after the 2018 NAO− event tend to occur indistinctly during winters with and without SSWs. In contrast, the NAO− event (+15/+35 days after the SSW, Figure 1c) displays a large drop in good circulation analogues (Figure 3d). This is an expected result given the exceptionality of the NAO− event, which means that there are no perfect analogues of this record-breaking event in the observational record. Still, the number of good analogues of the 2018 NAO− event is significantly ($p < 0.01$) higher in the pool of winter days that follow SSWs (i.e., such an exceptional event is more likely in winter with SSWs). Therefore, the observed synoptic conditions match better with those registered after SSWs, providing another piece of evidence of a stratospheric influence.

4. Concluding Remarks

The end of February 2018 was characterized by a sudden shift from a severe drought to record-breaking precipitation in March over the Iberian Peninsula. Two weeks earlier an outstanding SSW took place in the polar stratosphere. We have analyzed both events and employed a WRs approach to provide evidence of a connection between them.

Our results show that both Iberian precipitation and the SSW exhibited record-breaking signatures. Rainfall anomalies were the largest since 1979, associated with an extremely persistent NAO− event. The SSW featured a split of the polar vortex and was exceptional in terms of strength and persistence of the easterly winds in the middle stratosphere. The extratropical wave activity at 100 hPa that preceded the SSW was record-breaking, with the largest WN2 component on record. The evolution of the polar stratospheric state and the wave activity closely resembled very much that of the 2009 SSW, which had been identified as the strongest SSW in the observational period at the time (Ayarzagüena et al., 2011). The following key points confirm a link between the 2018 SSW and the end of the Iberian drought:

1. The SSW signal propagated downward reaching the troposphere timely with a tropospheric WR shift to NAO− and a sudden increase in precipitation.
2. The NAO− event after 2018 SSW was very persistent (21 days), consistent with the tendency for NAO− events to linger after SSWs.
3. The rainy conditions over Iberia after the 2018 SSW also agree with those observed under the influence of SSWs. Indeed, the probability of above-average Iberian precipitation conditioned on the occurrence of a SSW is significantly higher than the climatology.
4. Although the 2018 NAO− event displayed extraordinary features, the observed synoptic conditions are better reproduced by those occurring after SSWs than in the remaining pool of winter days.

Thus, we conclude that the stratosphere contributed to the establishment and persistence of the extreme conditions over southwestern Europe in March 2018. Although these conditions were record breaking (as some of the characteristics of the SSW were), qualitatively this event represents a clear example of the canonical tropospheric response to SSWs. Thus, it can serve as a guide for mechanistic studies analyzing in detail the stratosphere-troposphere dynamical coupling and ultimately help to improve seasonal forecast predictions.

Acknowledgments
B. A. and A. d. C. were funded by *Ayudas para la contratación de personal postdoctoral en formación en docencia e investigación en departamentos de la UCM*. M. A. is supported by the Programme Atracción de Talento de la Comunidad de Madrid (2016-T2/AMB-1405). J. M. G.-P. was supported by a predoctoral research grant awarded by the Spanish Ministerio de Educación, Cultura y Deporte (FPU16/01972). C. O. acknowledges funding from the Ramón y Cajal Programme of the Spanish Ministerio de Economía y Competitividad under grant RYC-2014-15036. We acknowledge support from the Spanish National Projects STEADY (CGL2017-83198-R) and PALEOSTRAT (CGL2015-69699) and the European Project 603557-STRATOCLIM under program FP7-ENV.2013.6.1-2. NCEP/NCAR Reanalysis and CPC Global Unified Precipitation data were provided by the NOAA/OAR/ESRL PSD, Boulder, Colorado, USA, from their Web site at https://www.esrl.noaa.gov/psd/. The authors would like to thank Judah Cohen and an anonymous reviewer.

References

Associaçao Portuguesa de Energias Renováveis (2018). March 100% renewable, first month of XXI century fully supplied by renewable electricity sources http://www.apren.pt/contents/communicationpressrelease/comunicado-apren-zero-marco-2018--en.pdf

Aurenhammer, F. (1991). Voronoi diagrams—A survey of a fundamental geometric data structure. *ACM Computer Surveys*, *23*(3), 345–405. https://doi.org/10.1145/116873.116880

Ayarzagüena, B., Langematz, U., & Serrano, E. (2011). Tropospheric forcing of the stratosphere: A comparative study of the two different major stratospheric warmings in 2009 and 2010. *Journal of Geophysical Research*, *116*, D18114. https://doi.org/10.1029/2010JD015023

Baldwin, M. P., & Dunkerton, T. J. (2001). Stratospheric harbingers of anomalous weather regimes. *Science*, *294*(5542), 581–584. https://doi.org/10.1126/science.1063315

Barriopedro, D., & Calvo, N. (2014). On the relationship between ENSO, stratospheric sudden warmings, and blocking. *Journal of Climate*, *27*(12), 4704–4720. https://doi.org/10.1175/JCLI-D-13-00770.1

Butler, A. H., Seidel, D. J., Hardiman, S. C., Butchart, N., Birner, T., & Match, A. (2015). Defining sudden stratospheric warmings. *Bulletin of the American Meteorological Society*, *96*(11), 1913–1928. https://doi.org/10.1175/BAMS-D-13-00173.1

Charlton, A. J., & Polvani, L. M. (2007). A new look at stratospheric sudden warmings. Part I: Climatology and modeling benchmarks. *Journal of Climate*, *20*(3), 449–469. https://doi.org/10.1175/JCLI3996.1

Charlton-Pérez, A. J., Ferranti, L., & Lee, R. W. (2018). The influence of the stratospheric state on North Atlantic weather regimes. *Quarterly Journal of the Royal Meteorological Society*, *144*(713), 1140–1151. https://doi.org/10.1002/qj.3280

Cohen, J., & Jones, J. (2011). Tropospheric precursors and stratospheric warmings. *Journal of Climate*, *24*(24), 6562–6572. https://doi.org/10.1175/2011JCLI4160.1

Corti, S., Molteni, F., & Palmer, T. N. (1999). Signature of recent climate change in frequencies of natural atmospheric circulation regimes. *Nature*, *398*(6730), 799–802. https://doi.org/10.1038/19745

Garcia-Herrera, R., Garrido-Perez, J. M., Barriopedro, D., Ordóñez, C., Vicente-Serrano, S. M., Nieto, R., et al. (2018). The severe drought of 2016–2017 in Western Europe, EGU General Assembly 2018, in *Geophysical Research Abstracts*, 20, EGU2018–8456-1.

Garfinkel, C. I., Hartmann, D. L., & Sassi, F. (2010). Tropospheric precursors of anomalous Northern Hemisphere stratospheric polar vortices. *Journal of Climate*, *23*(12), 3282–3299. https://doi.org/10.1175/2010JCLI3010.1

Gerber, E. P., Orbe, C., & Polvani, L. M. (2009). Stratospheric influence on the tropospheric circulation revealed by idealized ensemble forecasts. *Geophysical Research Letters*, *36*, L24801. https://doi.org/10.1029/2009GL04091

Hitchcock, P., & Simpson, I. R. (2014). The downward influence of stratospheric sudden warmings. *Journal of the Atmospheric Sciences*, *71*(10), 3856–3876. https://doi.org/10.1175/JAS-D-14-0012.1

Jézéquel, A., Cattiaux, J., Naveau, P., Radanovics, S., Ribes, A., Vautard, R., et al. (2018). Trends of atmospheric circulation during singular hot days in Europe. *Environmental Research Letters*, *13*(5), 054007. https://doi.org/10.1088/1748-9326/aab5da

Kalnay, M. E., Kanamitsu, M., Kistler, R., Collins, W., Deaven, D., Gandin, L., et al. (1996). The NCEP/NCAR 40-year reanalysis project. *Bulletin of the American Meteorological Society*, *77*(3), 437–471. https://doi.org/10.1175/1520-0477(1996)077<0437:TNYRP>2.0.CO;2

Karpechko, A. Y., Hitchcock, P., Peters, D. H. W., & Schneidereit, A. (2017). Predictability of downward propagation of major sudden stratospheric warmings. *Quarterly Journal of the Royal Meteorological Society*, *143*(704), 1459–1470. https://doi.org/10.1002/qj.3017

Kidston, J., Scaife, A. A., Hardiman, S. C., Mitchell, D. M., Butchart, N., Baldwin, M. P., & Gray, L. J. (2015). Stratospheric influence on tropospheric jet streams, storm tracks and surface weather. *Nature Geoscience*, *8*(6), 433–440. https://doi.org/10.1038/ngeo2424

MAPAMA Ministerio de Agricultura y Pesca, Alimentación y Medio Ambiente (2018). Boletín hidrológico semanal, 15.

Matsuno, T. (1971). A dynamical model of the stratospheric sudden warming. *Journal of the Atmospheric Sciences*, *28*(8), 1479–1494. https://doi.org/10.1175/1520-0469(1971)028<1479:ADMOTS>2.0.CO;2

Met Office (2018). March statistics may challenge your perception [online] Accessed 7 June 2018, https://www.metoffice.gov.uk/news/releases/2018/march-statistics

Michelangeli, P. A., Vautard, R., & Legras, B. (1995). Weather regimes: Recurrence and quasi stationarity. *Journal of the Atmospheric Sciences*, *52*(8), 1237–1256. https://doi.org/10.1175/1520-0469(1995)052<1237:WRRAQS>2.0.CO;2

Nishii, K., Nakamura, H., & Orsolini, Y. J. (2011). Geographical dependence observed in blocking high influence on stratospheric variability through enhancement and suppression of upward planetary-wave propagation. *Journal of Climate*, *24*(24), 6408–6423. https://doi.org/10.1175/JCLI-D-10-05021.1

National Oceanic and Atmospheric Administration (2018). National Centers for Environmental Information, state of the climate: Global climate report for March 2018, published online April 2018, retrieved on June 7, 2018 from https://www.ncdc.noaa.gov/sotc/global/201803

Palmeiro, F. M., Barriopedro, D., García-Herrera, R., & Calvo, N. (2015). Comparing sudden stratospheric warming definitions in reanalysis data. *Journal of Climate*, *28*(17), 6823–6840. https://doi.org/10.1175/JCLI-D-15-0004.1

Pedregosa, F., Varoquaux, G., Gramfort, A., Michel, V., Thirion, B., Grisel, O., & Vanderplas, J. (2011). Scikit-learn: Machine learning in Python. *Journal of Machine Learning Research*, *12*, 2825–2830.

Rosenblatt, M. (1956). Remarks on some nonparametric estimates of a density function. *The Annals of Mathematical Statistics*, *27*(3), 832–837. https://doi.org/10.1214/aoms/1177728190

The Guardian (2018). Sudden stratospheric warming set to bring lengthy cold snap to UK, [online], Accessed 28 June 2018, https://www.theguardian.com/uk-news/2018/feb/19/sudden-stratospheric-warming-set-to-bring-lengthy-cold-snap-to-uk

The Washington Post (2018). The 'beast from the east' just coated Rome in snow. Here's what it looks like, [Online], Accessed 7 June 2018, https://www.washingtonpost.com/news/capital-weather-gang/wp/2018/02/26/the-beast-from-the-east-just-coated-rome-in-snow-heres-what-it-looks-like/?noredirect=on&utm_term=.2433659e171b

Wilks, D. S. (2011). *Statistical methods in the atmospheric sciences* (3rd ed.). Oxford: Academic Press.

Xie, P., Chen, M., & Shi, W. (2010). CPC global unified gauge-based analysis of daily precipitation, Preprints, 24th Conf. on Hydrology, Atlanta, GA, Amer. Meteor. Soc, 2.